

Sol-gel TiO₂ nanoparticles prompt photocatalytic cement for pollution degradation

Elena Cerro-Prada^{*}, Vicente Torres Costa⁺ and Miguel Manso Silván⁺⁺

^{*}Civil Engineering Dept., Universidad Politécnica de Madrid, Spain, elena.cerro@upm.es

⁺Applied Physics Dept., Universidad Autónoma de Madrid, Spain, vicente.torres@uam.es

⁺⁺Applied Physics Dept., Universidad Autónoma de Madrid, Spain, miguel.manso@uam.es

Abstract TiO₂ nanoparticles (TiO₂NPs) prepared by the sol–gel method have been incorporated to cement paste with the aim of creating a photocatalytic system capable of compensating, through degradation of hazardous molecules, the environmental impact associated to the production of the clinker. Doping was carried out at different mass ratios with TiO₂NPs precursor solutions within a fresh cement paste, which was then characterized using scanning electron microscopy (SEM). The photocatalytic performance was evaluated by the degradation of Methylene Blue (MB) using a 125W UV lamp as irradiating source. Main cement properties such as hydration degree and C-S-H content are affected by TiO₂NPs doping level. Cement containing TiO₂NPs exhibited an increasing photocatalytic activity for increasing doping, while the pure cement paste control could hardly degrade MB. The kinetics of the system were also studied and their second order behavior related to microstructural aspects of the system.

1 Introduction

In order to address the significant problem of environmental pollution, extensive research is underway to develop advanced analytical, biochemical, and physicochemical methods for the characterization and degradation of hazardous chemical compounds from air, soil, and water. Advanced physicochemical processes such as semiconductor photocatalysis have been applied to a variety of problems of environmental interest in addition to water and air purification. Several simple oxide and sulfide semiconductors, such as TiO₂, ZnO or ZnS, have band-gap energies sufficient for promoting a wide range of chemical reactions of environmental interest. Among these semiconductors TiO₂ has proven to be the most suitable for widespread environmental applications. TiO₂ is biologically and chemically inert; it is stable with respect to photocorrosion and chemical corrosion; and, moreover, it is inexpensive.

Despite crystallinity is not the only key factor that determines the photocatalytic performance, titanium dioxide in anatase form appears to be the most photoactive and the most practical of the semiconductors for environmental applications [1]. However, many researchers claim that amorphous titania is also a catalytically active form of TiO_2 , exhibiting a selective activity toward certain substrates [2]. This study, among other, confirms that if an appropriate porous configuration is provided, the photocatalytic activity could be higher for amorphous structures, which leads to the conclusion that microstructural aspects play a significant role as well.

In the present work, it was attempted to present the photocatalytic performance of non-condensed TiO_2 nanoparticles (TiO_2NPs) prepared by sol-gel and inserted into the cement paste. The model dye chosen to establish the degradation capability was methylene blue (MB). The kinetics of the MB disappearance was studied. The influence of embedded TiO_2 precursors on the microstructure of the cementitious matrix was also analyzed.

2 Experimental

2.1 Materials

Cement paste was prepared with CEM I 42,5 ordinary Portland cement supplied by Portland Valderrivas, Madrid, Spain. The chemical composition was SiO_2 (20.80), Al_2O_3 (4.40), Fe_2O_3 (2.90), CaO (62.30), MgO (2.70), SO_3 (3.14) and the fineness was $1800 \text{ cm}^2/\text{g}$. The water/cement ratio used was 0.5. Methylene blue was supplied by Sigma-Aldrich at 0.04% solution in water and used as received. Solutions were prepared using de-ionized water with an initial concentration of $18 \times 10^{-6} \text{ M}$. The photocatalyst was TiO_2 sol prepared from the solution of titanium isopropoxide (TTIP) (97%) purchased from Sigma-Aldrich at 0.4 M in ethanol, with a precise TTIP/water molar ratio of 0.82 and pH of 1.27 controlled with HCl. TiO_2NP mean size = $14 \pm 7 \text{ nm}$ [3].

2.2 Photoreactor and light source

The photoreactor (90 ml) had a cylindrical shape with a top optical window whose section area was $\text{ca. } 11 \text{ cm}^2$, through which the suspension was irradiated. The UV-irradiation was provided by a high pressure UV 22 125 W mercury lamp (Optical Engineering) which emits radiation predominantly at 351 nm. In order to measure the absorption spectra of MB as a function of UV irradiation time, monochrome

(SpectraPro 150) transmitted light was measured with an SPD-M10Avp photodiode connected to a DSP dual lock-in amplifier (7225 Signal Recovery).

2.3 Procedure

Five series of TiO₂NPs-cement paste were prepared. The first series (CONTROL) consisted of pure cement paste stored at 293K in air, with no TiO₂ addition. The second to fifth series corresponded to cement paste mixed with TiO₂ sols. Four different TiO₂/cement paste content ratios were used, labeled TiO₂/CEM (1:10), (1:100), (1:1000) and (1:10000) according with their TiO₂/cement weight ratio. All samples were 1 cm×1 cm×0.3 cm in size. A volume of 100 ml of the aqueous solution of MB ($C_0 = 18 \times 10^{-6}$ M) was prepared and kept in the dark before using it. After the curing time, the cement specimens were inserted in 3 cm diameter quartz cuvettes filled with the aqueous dilution of MB. Samples were then irradiated with the UV lamp for different selected times, and their absorbance was measured.

3 Results and discussion

3.1 Photocatalytic degradation of MB in water by sol TiO₂NPs/cement/UV

The photocatalytic efficiency can be established by first-order kinetic equation using the basic equation of decay.

$$\ln(c/c_0) = -Kt \quad (1)$$

Where c_0 is the initial concentration of MB, c is the MB concentration at a given time t from which a decay constant K was calculated. This allows estimating a degradation rate calculated from fitting the kinetics of MB absorption to exponential decays. The values of the rate of degradation (μMmin^{-1}) were calculated from the kinetic data and plotted versus TiO₂ doping level, as shown in Figure 1. For the concentrations tested, it is observed that the degradation rate does not reach saturation for TiO₂NP additions, suggesting that there are still MB molecules available for degradation if an increased number of TiO₂NPs was incorporated. Thus, in the work presented herein, the degradation rate of MB increases with amount of photocatalyst without reaching a specific limit.

In order to examine the controlling mechanism of photodegradation process, the experimental data were also analyzed using the pseudo-first and pseudo-second-order kinetic models, and kinetic constants were calculated in all samples. The pseudo-first-order kinetic model has been widely used to predict dye degradation kinetics. A linear form of pseudo-first-order model was described by Lagergren.

$$\log(q_e - q) = \log q_e - (k_1 / 2.303)t \quad (2)$$

Where q_e and q are the amounts of photodegraded MB by the TiO₂NPs/Cement system at equilibrium and at time t , respectively (mg/g), and k_1 is the rate constant of first-order kinetics (1/min). The amount of photodegraded MB can be calculated from the experimental data by using the following relationship:

$$q_e = (c_0 - c_e)M \quad (3)$$

Where c_0 and c_e are the initial and equilibrium concentrations (mg/L) of MB, respectively, and M is the mass of TiO₂NPs used. The values of first-order rate constants and the correlation coefficient r^2 values obtained after the linear correlations were calculated. Although there is an initial increase in the k_1 from CONTROL sample to 1:10000 samples, only moderate increases are observed as the TiO₂NPs addition level increases, displaying even a lower equilibrium rate constant when the TiO₂/Cement weight rate reaches 1:100 levels. We found no applicability of the pseudo-first-order model in predicting the kinetics of MB absorption degradation in the TiO₂NPs doped cement paste was observed.

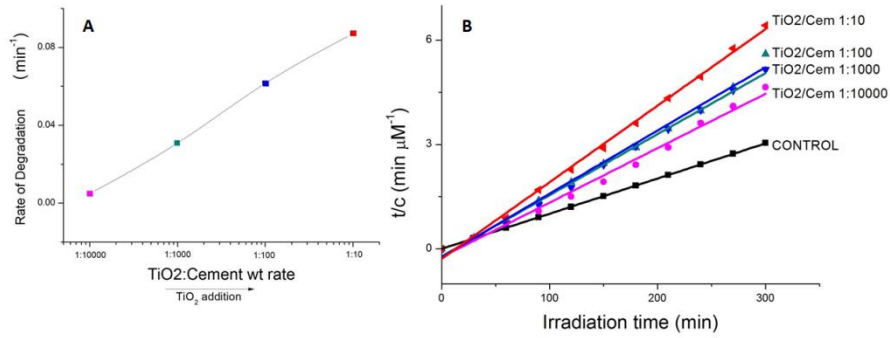


Fig. 1. (A) Speed of MB degradation versus TiO₂NPs doping level in TiO₂/Cement samples. (B) Pseudo-second-order kinetics approach for MB degradation in TiO₂NPs/Cement system at different addition levels

A pseudo-second-order model may also describe the kinetics of degradation. The pseudo second-order equation is based on the degradation capacity of the solid phase. This model predicts that intra-particle diffusion/transport process is the rate controlling step, which may involve valence forces through sharing or exchange of electrons between dye anions and photoreactants. The kinetic data were further analyzed using Ho's pseudo-second-order kinetics [4].

$$t/q = 1/(k_2 q_e) + (1/q_e)t \quad (4)$$

Where k_2 is the rate constant of second-order (1/min). If the second-order kinetic is applied, the plot of t/q against t should give a linear relationship, from which q_e and k_2 can be determined from the slope and intercept of the plot. The values were calculated from the kinetic data. The fitted plots are given in Figure 1b and the calculated q_e , k_2 , and the corresponding linear regression correlation coefficient values. The smallest correlation coefficient in this case was 0.98977, which corresponds to 1:10000 TiO₂/Cement weight ratio. The rest of the samples display correlation coefficients for the second-order kinetics model greater than 0.99, indicating the applicability of this kinetics equation and the second-order nature of the photodegradation process of MB in the TiO₂/Cement system. This fact indicates that the rate controlling step is intraparticle diffusion, which is in fact the kinetic mechanism followed by the hydration of anhydrous particles in the cement paste at the hydration period under examination [5].

3.2 Effects on cement microstructure

To obtain detailed information about the morphology of the TiO₂NPs/Cement system, SEM images were taken after 7 days of hydration for each specimen.

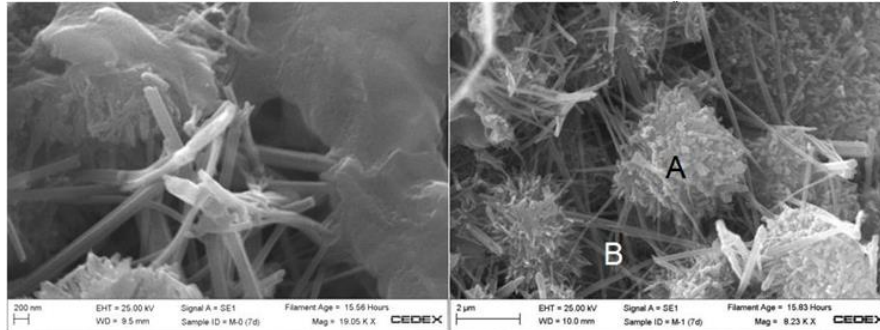


Fig. 2. Left: Detail of SEM micrograph of the CONTROL sample after 7 days hydration time (Right) and TiO₂/CEM 1:10 sample after 7 days hydration time, showing shell microspheres of amorphous inner C-S-H gel formed around a TiO₂ nanoparticle. Fibrillar outer C-S-H bridges the spherulites filling the intra-hydrate space

Significant contents of microspherulites were detected in all cement pastes doped with titania nanoparticles, as those shown in Figure 2 right, not found in the CONTROL sample (Figure 2 left).

A distinction between high density inner product and low density outer product can be established. The outer product shows morphology either fibrillar or foil like, whereas the inner product forms a pack and flocculates into what is usually termed “globule flocs”. The spherulitic morphology found in TiO₂NPs-cement samples, appears to be consisting of bundles of inner C-S-H gel diverging from a single TiO₂NP nucleus (A). Fibrillar outer C-S-H gel (B) bridges the spherulites, developing a network-like morphology. Although such spherulites were present in all TiO₂NPs/CEM samples, C-S-H gel with a foil-like morphology was observed to prevail with decreasing TiO₂NPs concentration.

4 Conclusions

TiO₂NPs were successfully synthesized by the sol-gel method and inserted in the cement paste along with the hydration water. SEM observations revealed that sol-gel TiO₂NPs were preferentially located in the porous structure of the cement, forming nucleation centers for the C-S-H gel development. The photocatalytic activity of the TiO₂NPs/cement system was measured as the relative change in the absorption of the methylene blue immersion solution. Our results clearly indicated that the TiO₂NPs/cement system is photoactive and the highest photocatalytic activity was obtained under the proportion: 1 part of TiO₂NPs over 10 parts of cement paste, in mass. The rate controlling step for the photocatalytic processes is intraparticle diffusion, which is in fact the kinetic mechanism followed by the hydration of anhydrous particles in the cement paste.

References

1. Sclafani A., Herrmann J. M. (1996). Comparison of the photoelectronic and photocatalytic activities of various anatase and rutile forms of titania in pure liquid organic phases and in aqueous solutions. *J. Chem. Phys.*, 100(32):13655-13661
2. Tao H. J., Tao J., Wang T et al (2005). Fabrication of self-organized TiO₂ nanotubes by anodic oxidation and their photocatalysis. *T. Nonferr Metal Soc.*, 15(3):462
3. Vaquero V. S., Noval A. M., Sánchez N. T. et al (2010). Preparation, modification and cellular evaluation of PEG-PEGd supports with titania nanoparticle loads. *Surf. Interface Anal.*, 42(6-7):481-485
4. Vadivelan V., Kumar K. V. (2005). Equilibrium, kinetics, mechanism, and process design for the sorption of methylene blue onto rice husk. *J. Colloid Interf. Sci.*, 286(1):90-100
5. Van Breugel K. (1995). Numerical simulation of hydration and microstructural development in hardening cement-based materials:(II) applications. *Cem. Concr. Res.*, 25(3):522-530